



Pregnancy-Associated Renal Cortical Necrosis and Nonenhanced Functional Magnetic Resonance Imaging: A Case Series

Rui Wang, Xiang Liu, Wei Li, Ying Tan, Jianxing Qiu, and Tao Su

Rationale & Objective: Pregnancy-associated renal cortical necrosis is a critical illness with a poor prognosis. We aimed to describe the clinical and magnetic resonance imaging (MRI) characteristics of a case series of patients with acute kidney injury in the setting of pregnancy-associated renal cortical necrosis.

Study Design: Case series.

Setting & Participants: Seventeen patients from a single center diagnosed by nonenhanced functional MRI and/or kidney pathology.

Results: All patients presented with postpartum acute kidney injury stage 3. Of the 17 patients, 15 (88%) had pregnancy-associated atypical hemolytic uremic syndrome, 11 (65%) had postpartum hemorrhage, 7 (41%) had preeclampsia/hemolysis elevated liver enzymes low platelet count syndrome, and 4 (24%) had disseminated intravascular coagulation. On T2-weighted MRI, the diffuse phenotype showed outer cortex swelling in the early phase, with a dark signal rim involving the inner cortex and

Bertin column, which became more apparent over time along with cortical thinning, substantially decreasing T2 signal intensity. The focal phenotype showed focally distributed hypointense signals in the cortex. After 8-101 (median: 60) months of follow-up, 4 individuals had estimated glomerular filtration rates ≥ 60 mL/min/1.73 m², 6 had estimated glomerular filtration rates of 15-60 mL/min/1.73 m², and 7 had kidney failure requiring kidney replacement therapy. The diffuse phenotype was present in all of the individuals who remained kidney replacement therapy dependent.

Limitations: Retrospective study; small sample size.

Conclusions: Different forms of pregnancy-associated thrombotic microangiopathy were the major causative diseases in our pregnancy-associated renal cortical necrosis case series. Nonenhanced functional MRI may provide valuable data for establishing diagnosis and kidney prognosis.

Complete author and article information provided before references.

Correspondence to T. Su (tao.su@bjmu.edu.cn)

Kidney Med. 5(5):100623. Published online March 8, 2023.

doi: 10.1016/j.xkme.2023.100623

© 2023 The Authors. Published by Elsevier Inc. on behalf of the National Kidney Foundation, Inc. This is an open access article under the CC BY-NC-ND license (<http://creativecommons.org/licenses/by-nc-nd/4.0/>).

Cortical necrosis is one of the most severe manifestations of pregnancy-associated acute kidney injury (AKI).¹ Obstetric complications, including postpartum hemorrhage, eclampsia, abruptio placentae, puerperal sepsis, septic abortion, and atypical hemolytic uremic syndrome (aHUS), are considered the major causes of pregnancy-associated renal cortical necrosis in developing countries.^{2,3} Pregnancy-associated renal cortical necrosis occurs in 1.5%-4.5% of pregnancy-associated AKI cases in developed countries and occurs more frequently (1%-17%) in developing countries.¹⁻⁴ It is characterized by ischemic destruction of the kidney cortex caused by a sudden but prolonged decrease in kidney arterial perfusion due to vascular spasm, microvascular injury, or intravascular coagulation.⁵ However, the exact pathogenesis of cortical necrosis in obstetric settings remains unclear.³ It often leads to severe sequelae, including kidney failure requiring replacement therapy (KFRT).⁶

Histopathological examination by kidney biopsy remains the gold standard for diagnosing cortical necrosis. However, kidney biopsies are invasive and may be contraindicated in many critically ill patients. Furthermore, kidney biopsies inevitably have sampling biases. Therefore, noninvasive imaging methods are essential for evaluating patients with cortical necrosis.

Contrast-enhanced computed tomography, magnetic resonance imaging (MRI), and angiography are the recommended diagnostic techniques for cortical necrosis.⁷⁻¹⁰ However, these contrast-based strategies have limitations when used in patients with kidney injury. There is an additional risk of aggravating AKI due to exposure to iodinated contrast media in arteriography and enhanced computed tomography.¹¹ Moreover, the potential risk of nephrogenic systemic fibrosis may limit the use of gadolinium-based contrast media in enhanced MRI.¹² Nonenhancement of the kidney cortical rim with simultaneous enhancement of the medulla, known as the “reverse rim sign,” is considered a characteristic sign of cortical necrosis.⁷⁻¹⁰ It has also been recommended for diagnosing cortical necrosis and assessing the disease severity.

Diffusion-weighted imaging (DWI) as a nonenhanced MRI sequence is sensitive to local water motion in the tissue. An overview of human studies applying kidney DWI in diffuse pathologies demonstrates the feasibility and intra-study reproducibility of DWI. These studies also emphasize the potential of apparent diffusion coefficient (ADC) value, a DWI-derived parameter, as a surrogate biomarker for interstitial fibrosis in chronic kidney disease and inflammation in AKI.¹³⁻¹⁵ This study aimed to describe the clinical and MRI features of pregnancy-associated renal

PLAIN-LANGUAGE SUMMARY

Pregnancy-associated renal cortical necrosis is a severe disorder with a poor kidney prognosis. We describe 17 patients with pregnancy-associated renal cortical necrosis. All patients presented with acute kidney injury stage 3. Different forms of thrombotic microangiopathy, including pregnancy-associated atypical hemolytic uremic syndrome and preeclampsia/hemolysis elevated liver enzymes low platelet count syndrome, were the major causative diseases contributing to cortical necrosis. Kidney function significantly improved in more than half of affected women during follow-up. Patients with kidney failure requiring replacement therapy at the last follow-up (> 6 months postpartum) had a more prevalent diffuse phenotype on T2-weighted images and a higher negative corticomedullary apparent diffusion coefficient difference. Nonenhanced functional magnetic resonance imaging may provide important information in the diagnosis of cortical necrosis and assessment of kidney outcome.

cortical necrosis and describe longer-term kidney outcomes.

METHODS

Study cohort

This retrospective analysis included patients with pregnancy-associated renal cortical necrosis admitted to the nephrology department of the Peking University First Hospital between January 2010 and December 2021. The inclusion criteria were as follows: (1) obstetric patients; (2) a definite diagnosis of cortical necrosis by kidney histopathology or a probable diagnosis of cortical necrosis based on typical history, clinical course, and radiographic findings; and (3) follow-up for >6 months. Patients without kidney MRI scans were excluded from the study. All patients provided written informed consent. This retrospective study complied with the principles of the Declaration of Helsinki. The Ethics Committee of the Peking University First Hospital approved the study protocol (2017[1280]).

Clinical information was collected from the electronic medical record system of our hospital, including age, gestational age, prior pregnancies, history of chronic hypertension, chronic kidney disease, diabetes mellitus or gestational diabetes mellitus, and lupus, and pregnancy complications including preeclampsia, hemolysis elevated liver enzymes low platelet count (HELLP) syndrome, postpartum hemorrhage, aHUS, and disseminated intravascular coagulation (DIC). Laboratory data recorded included peak serum creatinine, lactate dehydrogenase, albumin, hemoglobin, platelet count, complement C3 and C4 levels, factor H, and a disintegrin and metalloproteinase

with thrombospondin type 1 repeats, member 13 activity. We also evaluated the coagulation state by measuring the prothrombin time, activated partial thromboplastin time, fibrinogen, and D-dimer levels. DIC was defined as a high D-dimer level associated with 1 major criterion (platelet count $<50 \times 10^9/L$ or prothrombin time activity $<50\%$) or 2 minor criteria (platelet count ranging from $50-100 \times 10^9/L$, and/or prothrombin time activity from $50\%-100\%$, and/or fibrinogen <1 g/L). Oliguria and anuria were defined as daily urine volumes <500 or <50 mL, respectively. AKI was diagnosed according to the Kidney Disease: Improving Global Outcomes (KDIGO) diagnosis criteria.¹⁶

Functional MRI protocol

MRI was performed using phased-array body coils of Signa Excite HD 1.5 T (GE Medical System), Magnetom Area 1.5 T (Siemens), Ingenia 3.0 T (Philips Medical Systems), and Discovery MR750 3.0T (GE Medical System) scanners. Coronal T2-weighted images (T2WIs), axial T1-weighted images, fat saturation T2WIs, and DWIs were collected in each MRI scan. The detailed MRI parameters are presented in Table S1. The axial T2WI and DWI scans were coregistered beforehand. We used 2 b-values: 0/50 and 800 s/mm². The MRI images were first assessed by one radiologist with 10 years of experience, then by another radiologist with >20 years of experience in kidney radiological imaging. Both radiologists were blinded to the clinical data and made diagnoses separately. Based on the T2WI findings, patients were divided into diffuse imaging phenotype (the percentage of cortical lesion area $>75\%$) and focal imaging phenotype (the percentage of cortical lesion area $\leq 75\%$) groups by the 2 radiologists independently.

The ADC map was generated on an AW 4.6 workstation (General Electric Medical Systems) or the MRI scanners automatically. The readers were blinded to the clinical information of the patients. First, the cortical area was delineated layer by layer on axial T2WIs and summed to obtain the total cortical area (Fig S1A). Meanwhile, regions of interest (ROIs) were copied on the ADC map. The cortical ADC values were generated and recorded as the mean ADC values of the total cortical ROIs. Three ROIs, approximately 20 mm² in each area, were carefully placed in the medulla of the upper, middle, and lower poles of bilateral kidneys on axial T2WI and copied on the ADC map. The medullary ADC values were generated and recorded as the mean ADC values of the 6 ROIs. The corticomedullary difference (Δ ADC), which has been reported in previous studies as a valuable parameter to reduce inter-subject variability and predict the kidney outcome, was defined as (cortical ADC – medullary ADC).¹⁴ Then, ROIs were carefully placed in the cortex covering all lesions with decreased ADC values (Fig S1B) to yield the cortical lesion areas and values on the ADC map. The percentage of the cortical lesion area was calculated as (the sum of the cortical lesion area on the ADC map

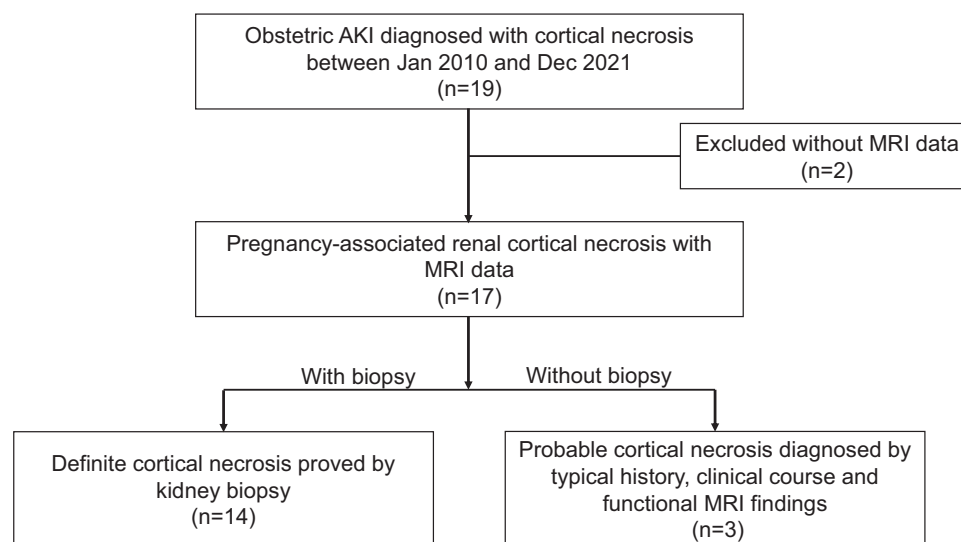


Figure 1. Flowchart of pregnancy-associated renal cortical necrosis patient recruitment. AKI, acute kidney injury; MRI, magnetic resonance imaging.

divided by the total cortical area). The lesion Δ ADC was defined as (mean cortical lesion ADC – medullary ADC).

Kidney Pathology

Kidney tissues were routinely stained using hematoxylin-eosin, Masson’s trichrome, periodic acid–Schiff, and periodic acid–silver methenamine staining for light microscopy examination. The tissue core was often obtained at a depth of approximately 1 cm. The severity of cortical necrosis was semi-quantitatively assessed as scores 1, 2, and 3, corresponding to a cortical necrosis area of <25%, 26%–50%, and >50% (mild, moderate, and severe), respectively, and evaluated by 2 experienced pathologists.

Kidney Outcomes

Each patient was followed by the clinic or via telephone interview. During follow-up, kidney function was evaluated by estimated glomerular filtration rate (eGFR) using the 4-variable Modification of Diet in Renal Disease Study equation.¹⁷ We classified patients as subgroups of eGFR ≥ 60 , 15–60, and <15 mL/min/1.73 m² or KFRT according to the eGFR at the last follow-up. The clinical, laboratory, and MRI-derived parameters of the subgroups were described to explore the potential factors for kidney outcomes.

Statistical Analyses

All statistical analyses were performed using SPSS (version 23.0; SPSS). Continuous variables are expressed as mean \pm standard deviation or median and interquartile range (IQR), according to the distribution, and categorical variables are expressed as percentages. Agreements on T2WI phenotypes evaluated by 2 radiologists and pathological scores evaluated by 2 pathologists were determined using κ statistics.

RESULTS

Clinical and Pathological Characteristics

Overall, 17 hospitalized patients with pregnancy-associated renal cortical necrosis were included in this study (Fig 1). Tables 1 and 2 present the obstetric features, clinical features, laboratory data, kidney histological findings, and nonenhanced MRI parameters of the 17 patients. The median gestational age at the time of pregnancy termination was 37 (IQR, 32–39) weeks. Eight patients (47.1%) had a history of repeated pregnancies, and 4 (23.5%) delivered twins. Of the 17 patients, 7 patients (41.2%) reported a history of preeclampsia, and 2 (11.8%) reported HELLP syndrome during the antenatal period. Eleven patients (64.7%) had a postpartum hemorrhage, 15 (88.2%) had pregnancy-associated aHUS, and 4 (23.5%) had DIC. All patients presented with postpartum AKI stage 3. Anuria and oliguria were reported in 13 (76.5%) and 4 (23.5%) patients, respectively (Table 1).

Definite cortical necrosis was pathologically proven via kidney biopsy in 14 (82.4%) patients, 7 of whom had severe (>50%) cortical necrosis whereas the other 7 had mild (<25%) cortical necrosis. Coagulative necrosis was distinctive, involving the majority of tubular segments and glomeruli under light microscopy observation. Nuclei appeared pale and pyknotic or were no longer apparent. Typical signs of TMA were disclosed in all 14 patients manifesting as obvious endothelial cell swelling, thrombi in the microcirculation, and a “double contours” aspect of the glomerular basement membrane. Excellent agreement was noticed on pathological scores between 2 pathologists ($\kappa = 0.86$). Three patients (P12, 13, 15) were identified as having probable cortical necrosis based on the typical history, clinical course, and functional MRI findings.

Table 1. Clinical characteristics and laboratory data of the 17 patients with pregnancy-associated renal cortical necrosis.

Patient No.	1	2	3	4	5	6	7	8	9	10	11	12	13	14	15	16	17
Clinical features																	
Age, y	25	33	30	27	31	31	34	27	28	26	32	33	32	38	39	35	27
Gestational age, wk	35	34	40	37	38	41	37	31	42	38	34	40	38	7	17	33	31
Pregnancy history	G2P1	G1P1	G2P1	G1P1	G2P3	G1P1	G1P2	G1P1	G1P1	G1P2	G2P3	G4P1	G1P1	G5P2	G2P1	G2P1	G1P1
Other adverse pregnancy outcomes	–	–	IFD*	–	SA	–	–	–	–	–	–	ED	–	–	–	–	FD
Twin pregnancy	–	–	–	–	+	–	+	–	–	+	+	–	–	–	–	–	–
Underlying diseases																	
Diabetes mellitus	–	–	–	–	–	–	–	–	–	GDM	–	–	–	–	–	GDM	–
Etiology of AKI																	
Preeclampsia	–	+	–	+	+	–	+	+	–	–	+	–	–	–	–	+	–
HELLP syndrome	–	–	–	–	–	–	–	+	–	–	–	–	–	–	–	+	–
Postpartum hemorrhage	–	–	+	–	–	+	+	+	+	–	–	+	+	+	+	+	+
aHUS	+	+	+	+	+	+	+	+	+	+	+	–	+	+	–	+	+
DIC	–	–	+	–	–	–	–	–	–	+	–	–	–	+	+	–	–
AKI stage	3	3	3	3	3	3	3	3	3	3	3	3	3	3	3	3	3
Plasmapheresis	+	+	+	+	+	+	–	+	+	+	+	–	+	–	+	+	+
No. of plasmapheresis sessions	6	3	7	6	5	4	NA	17	7	8	9	NA	3	NA	5	10	7
Oliguria/anuria	O	A	O	A	A	A	A	A	A	A	A	A	A	O	A	A	O
MAP at onset, mm Hg	117	150	91	123	140	100	98	130	108	107	120	123	107	92	47	121	90
MAP at the time of biopsy, mm Hg	100	103	89	99	88	84	86	123	110	93	98	NA	NA	77	NA	112	90
MAP at the time of MRI, mm Hg	102	103	99	110	102	120	96	113	89	110	106	97	104	74	83	99	92
Laboratory data at onset																	
Hemoglobin, g/L (115-150 g/L)	82	78	75	93	111	73	65	69	72	101	86	95	87	79	72	109	74
LDH, IU/L (100-240 IU/L)	1281	1679	258	3449	2620	2485	1447	1398	2250	2376	1826	NA	726	696	958	665	1285
Platelet count, $\times 10^9/L$ (125-350 $\times 10^9/L$)	356	105	203	79	52	79	22	46	27	120	96	39	86	793	79	74	57
Alanine aminotransferase, IU/L (7-40 IU/L)	33	77	78	71	82	8	19	15	252	63	7	N**	N**	NA	13	11	41
Aspartate aminotransferase, IU/L (13-35 IU/L)	42	55	139	279	312	17	103.8	80	133	227	18	N**	235	NA	19	18	59
Hematuria	+	+	+	+	+	–	NA	+	+	+	+	NA	–	+	NA	NA	+
C3, g/L (0.6-1.5 g/L)	0.92	1.08	N**	0.95	0.88	0.76	1.14	0.67	0.68	1.33	0.61	0.74	NA	1.01	0.56	0.54	0.57
C4, g/L (0.12-0.36 g/L)	0.17	0.4	N**	0.17	0.32	0.26	0.26	0.07	0.28	0.48	0.14	0.21	NA	0.27	0.11	0.12	0.11
Factor H, μ g/mL (247-1010.8 μ g/ml)	NA	619.8	553.3	666.3	471.3	582.5	496.5	439.8	399.6	646.5	NA	528	327.5	402	381.1	356	655.2
ADAMTS13 activity, % (40%-99%)	NA	74	87	91	85	78	68	59	88	88	NA	92	92	75	89	72	89
D-dimer, mg/L (<0.24 mg/L)	0.71	1.04	2.61	2.44	1.2	3.36	0.24	1.25	0.79	1	2.41	0.55	49.02	3.2	1.07	2.02	9.65
Prothrombin time, s (10.1-12.6 s)	10.1	10.2	10.9	15.4	12.2	12	11.2	9.8	11.2	11.1	12.7	10.4	13	13.6	14	11.9	10.9
Activated partial thromboplastin time, s (26.9-37.6 s)	36.3	30.8	28.3	34.9	31.5	30.3	33.8	21.2	31.4	25.6	29.4	36.8	29.5	27.9	26.9	25.6	29.1
Fibrinogen, g/L (2-4 g/L)	3.31	3.01	4.32	5.43	3.58	3.03	3.96	1.32	2.3	2.02	2.48	2.73	1.7	7.26	1.88	1.79	2.72

Abbreviations: ADAMTS13, a disintegrin and metalloproteinase with thrombospondin type 1 repeats, member 13; aHUS, atypical hemolysis uremic syndrome; AKI, acute kidney injury; DIC, disseminated intravascular coagulation; ED, embryo damage; FD, fetal death; GDM, gestational diabetes mellitus; HELLP, hemolysis, elevated liver enzymes, and low platelet count; IFD*, intrauterine fetal death due to umbilical cord around the neck; LDH, lactate dehydrogenase; MAP, mean arterial pressure; MRI, magnetic resonance imaging; N**, normal range; NA, not available; SA, spontaneous abortion.

Table 2. Pregnancy-associated characteristics and kidney outcomes of the 17 patients with pregnancy-associated renal cortical necrosis.

Patient No.	1	2	3	4	5	6	7	8	9	10	11	12	13	14	15	16	17
Pregnancy-associated renal cortical necrosis characteristics																	
Duration from delivery to biopsy, wk	3	4.1	5.9	6.7	5.3	6.3	20	7.3	6.7	3	4.3	NA	NA	6.3	NA	3.0	2.6
Biopsy-proven (diffuse type [DI]: >50%/focal type [FI]: <25%)	D	D	D	F	F	F	D	D	D	F	F	NA	NA	F	NA	D	F
Duration from delivery to MRI, wk	4.7	3.3	6.1	1.3	4.9	2.3	18.7	7.1	7	3.3	2.4	11	6.6	7.4	4	1.6	1.4
T2WI phenotypes (diffuse type [DI]: >75%/focal type [FI]: ≤75%)	D	D	D	D	F	D	F	D	D	F	F	D	D	F	D	D	F
Lesion area percentage on the ADC map	18%	16%	6%	11%	2%	24%	5%	18%	20%	3%	1%	18%	26%	3%	39%	7%	3%
Negative ΔADC value, 10 ⁶ mm ² /s	383.68	358.19	287.04	240	77.78	276.27	159.47	338	214	129.72	3.62	390.82	349.36	152.07	163.61	170.46	68.97
Sum of (the negative lesion ΔADC × the corresponding lesion area)	0.63	0.59	0.16	0.66	0.07	0.79	0.12	0.37	0.26	0.06	0.02	0.24	0.8	0.04	0.26	0.24	0.16
Kidney outcome																	
eGFR at the last follow-up, mL/min/1.73 m ²	KFRT	KFRT	KFRT	KFRT	72.21	48.26	55.21	KFRT	KFRT	KFRT	74.03	65	KFRT	16.09	31.27	KFRT	28.11
Follow-up, mo	101	88	70	67	66	57	45	33	29	20	53	64	66	60	29	8	65

Abbreviations: ADC, apparent diffusion coefficient; eGFR, estimated glomerular filtration rate; KFRT, kidney failure requiring replacement therapy; MRI, magnetic resonance imaging; NA, not available; T2WI, T2-weighted image.

Functional MRI Features

All 17 patients underwent kidney nonenhanced functional MRI proximate to kidney biopsy (median, 7.5; IQR, 2-12 days). The median MRI time was 33 (IQR, 17-50) days postpartum. Two patients underwent serial MRI at either 1 (P6, 16) or 3 months (P6) after the first MRI scan or both. All patients were confirmed to have cortical necrosis based on nonenhanced functional MRI findings by 2 radiologists.

Table 3 summarizes the kidney MRI findings of the 17 obstetric patients with cortical necrosis. The classification of imaging phenotypes on T2WI assessed by the 2 radiologists was completely consistent ($\kappa = 1$). Eleven patients (64.7%) were identified as having the diffuse phenotype, and the other 6 (35.3%) were identified as having the focal phenotype of cortical necrosis. Patients with the diffuse phenotype had multiple hypointense signal lesions in the cortex. They showed swelling of the outer cortex in the early phase, with a dark signal rim involving the inner cortex and column of Bertin (Fig 2A); however, these were not obvious in patients with the focal phenotype. The dark signal rim became more apparent over time, along with cortical thinning and a substantial decrease in T2 signal intensity in the chronic phase (Fig 2B). Compared with the normal cortex, relatively higher signal intensity was noted on the T2WIs of 2 patients (P4, 16) who underwent MRI scans 9 and 11 days after the disease flare (Fig 2A). Serial MRI revealed shrinkage of the swollen cortex contour at 1 month (Fig 2B) despite the recovery of kidney function. The 6 patients with the focal phenotype also had focally distributed hypointense signals in the cortex on T2WIs (Fig 3). Two patients (P17, 11) who underwent MRI 10 and 17 days postpartum presented mild changes in the kidney cortex contour; however, the other 4 patients had varying degrees of cortical lesion thinning. Although focal changes in the hypointense signal in the cortex and column of Bertin were detected on the ADC map, they were milder than those on the T2WIs (Fig 4).

Kidney Outcomes

Of the 17 patients, 4 (23.5%) had restored kidney function to eGFR ≥ 60 mL/min/1.73 m², 6 (35.3%) had eGFR 15-60 mL/min/1.73 m², and 7 (41.2%) had KFRT at the last follow-up (8-101 months, median 60 months). Fourteen patients (82.4%) underwent therapeutic plasmapheresis. The percentage of patients receiving plasmapheresis was 100%, 66.7%, and 85.7% in eGFR ≥ 60 mL/min/1.73 m², 15-60 mL/min/1.73 m², and KFRT outcome subgroups, respectively. The median session was 6.5 (IQR, 4.8-8.3) times. Patients with eGFR ≥ 60 mL/min/1.73 m² underwent more sessions of plasmapheresis (median, 7.5; IQR, 5.5-8.8 times) than patients with eGFR 15-60 mL/min/1.73 m² (median, 5.5; IQR, 3.3-9.3 times) and KFRT (median, 6; IQR, 4.5-9.5 times). No death or other organ failure, such as uncontrolled cardiac dysfunction, was noted. Four patients (P5, 10, 11, 17) finally recovered to eGFR >60 mL/min/1.73 m² with a median duration of 4.5 (IQR, 2.3-6) months.

Table 3. MRI characteristics of diffuse and focal imaging phenotypes in patients with pregnancy-associated renal cortical necrosis.

	Diffuse type (n = 11)	Focal type (n = 6)
T2WI		
Hypointense signal of the cortical lesions	11/11, diffuse	6/6, focal or patchy
Dark signal rim along the inner cortex and the column of Bertin	11/11	0/6
Swelling with hyperintense signal of the outer cortex	2/11	0/6
Thinning or atrophy of the cortical lesion	8/11	4/6
ADC map		
Hypointense signal of the cortical lesion	11/11, focal	6/6, focal

Abbreviations: ADC, apparent diffusion coefficient; MRI, magnetic resonance imaging; T2WI, T2-weighted image.

The prevalence of diffuse type cortical necrosis on T2WI was 0%, 66.7%, and 100% in the eGFR ≥ 60 mL/min/ 1.73 m², 15-60 mL/min/ 1.73 m², and KFRT outcome subgroups, respectively. The percentage of the cortical lesion area on the ADC map was significantly higher in the KFRT subgroup ($20\% \pm 8.85\%$) than in the eGFR ≥ 60 mL/min/ 1.73 m² ($2.25\% \pm 0.96\%$) and eGFR 15-60 mL/min/ 1.73 m² ($11.83\% \pm 10.3\%$) subgroups. The negative Δ ADC value of the KFRT subgroup ($298.33 \pm 90.98 \times 10^{-6}$ mm²/s) was greater than that of the eGFR ≥ 60 mL/min/ 1.73 m² subgroup ($70.02 \pm 51.75 \times 10^{-6}$ mm²/s) and eGFR 15-60 mL/min/ 1.73 m² subgroup ($232.45 \pm 82.7 \times 10^{-6}$ mm²/s). Furthermore, the sum of (the negative lesion Δ ADC \times the corresponding lesion

area) of the KFRT subgroup (0.37; IQR, 0.26-0.63) was higher than that of the eGFR ≥ 60 mL/min/ 1.73 m² (0.07; IQR, 0.03-0.14) and eGFR 15-60 mL/min/ 1.73 m² subgroups (0.2; IQR, 0.1-0.79) (Table 1).

DISCUSSION

In this case series of 17 patients with pregnancy-associated renal cortical necrosis from a single center, we demonstrated a prevalence of 88.2% for aHUS, 64.7% for postpartum hemorrhage, 41.2% for preeclampsia/HELLP syndrome, and 23.5% for DIC based on the clinical and histological findings. This result contrasts from prior reports. In the past, pregnancy-associated renal cortical necrosis was thought to be majorly associated with massive hemorrhage caused by placenta previa, abruptio placentae, postpartum hemorrhage, or other severe complications such as amniotic fluid embolism and septic abortions.^{2,18,19} However, various presentations of TMA during pregnancy- and postpartum-induced cortical necrosis may have been underdiagnosed.^{3,6} The spectrum of pregnancy-associated TMA includes preeclampsia/HELLP syndrome, acute fatty liver, and aHUS/thrombotic thrombocytopenic purpura.^{20,21} Based on the results of our study, aHUS and preeclampsia/HELLP syndrome were the major causative diseases contributing to cortical necrosis, in addition to postpartum hemorrhage and DIC. We also reported better long-term kidney outcomes than previous prognostic studies in developing countries,^{3,6} with more than half of patients with renal cortical necrosis not dependent on kidney replacement therapy at follow-up.

Our findings of nonenhanced functional MR image features supported that the dark signal rim at the inner cortex and Bertin column with swelling of the outer cortex on T2WI were early signs of cortical necrosis. However, we found that the dark signal rim at the inner cortex and

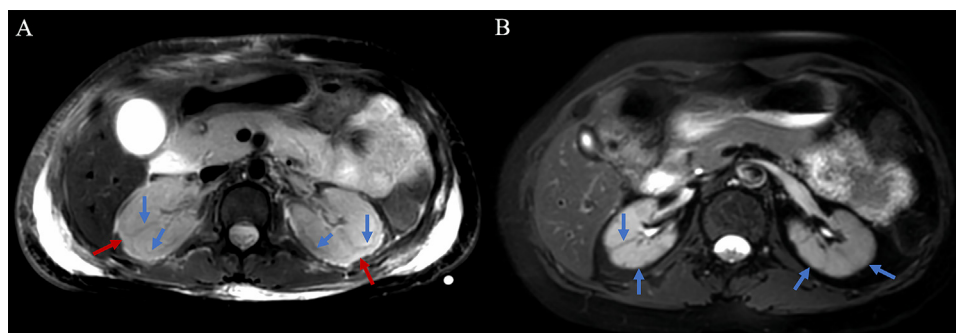


Figure 2. A 35-year-old woman presented with preeclampsia/hemolysis elevated liver enzymes low platelet count (HELLP) syndrome, and postpartum hemorrhage due to abruptio placentae. She terminated her pregnancy at 33 weeks of gestation. After delivery, she had acute kidney injury and was identified with atypical hemolysis uremic syndrome (aHUS). T2-weighted imaging (A) conducted on the 11th day after delivery demonstrated that the dark signal rim was in the inner cortex and along the column of Bertin (blue arrows) with swelling outer cortex and relatively high signal intensity (red arrows). She was identified in the early phase of diffuse type of cortical necrosis. The T2-weighted image (B) obtained on day 41 after delivery demonstrated both kidneys were shrunken, and the dark signal rim of the cortex and column of Bertin (blue arrows) were much more apparent.

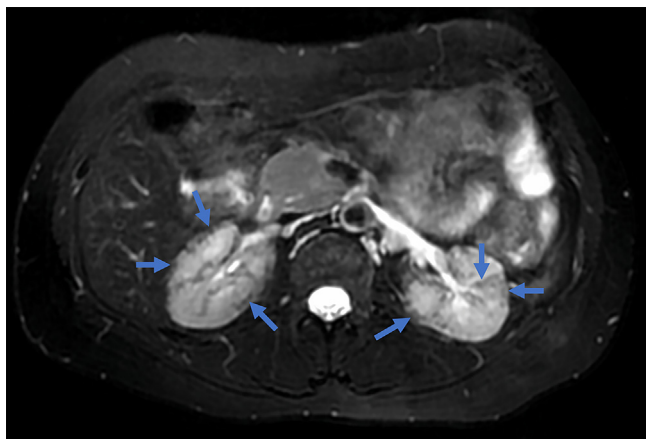


Figure 3. A 31-year-old woman, who delivered twins, presented with preeclampsia and postpartum acute kidney injury and was diagnosed with atypical hemolysis uremic syndrome (aHUS). The T2-weighted image obtained on the 34th day after delivery demonstrated a patchy hypointense signal in the cortex and the column of Bertin.

the Bertin column became more apparent over time, along with cortical thinning and substantially decreasing T2-weighted signal intensity, indicating the insidious progression of the acute-to-chronic transition. Neither the dark signal rim at the inner cortex and Bertin column nor the outer cortex swelling was detected in the 6 patients with the focal phenotype. A previous study reported a close relationship between dark signal intensity rim at the inner cortex and Bertin column and either calcification, fibrosis, or both, in the chronic phase, which was confirmed by computed tomography imaging and kidney biopsy.⁹

The exact pathogenic mechanism of pregnancy-associated renal cortical necrosis remains unclear. Ischemic destruction of the kidney cortex may result from severe but consistent kidney hypoperfusion, vascular endothelial injury, and the release of proinflammatory and procoagulant factors.²² The inner cortex and Bertin column regions were more vulnerable to ischemia than the subcapsular outer cortex and medulla regions. Although the renal cortex receives 20%-25% of cardiac output and the medulla receives a mere 10% of the cortical blood flow,²³ the cortex and medulla underlie different blood flow controls. The kidney regional differences in vascular architecture and geometry may predispose medullary blood flow to be relatively insensitive to most vasoconstrictor factors.²⁴ The perfusion of the cortex decreased dramatically with a ratio of 2.1 (compared to a ratio of 6.6 at rest) under hypovolemic shock with the promptly initiated redistribution of intrarenal microcirculation in animal studies.²⁵⁻²⁷ The subcapsular outer cortex can be saved because of the extra blood supplied by the capsular arteries. We hypothesize that the swelling of the cortex with hyperintense signals is caused by congestion in the acute phase because of the reduced number of functional glomeruli and subsequent disorders of water molecule filtration and tubular reabsorption. The onset of kidney calcification and fibrosis after severe cortical necrosis is marked by cortical thinning, shrinkage, and decreased signal intensity on T2WI.

The gold standard for diagnosing cortical necrosis still relies on histopathological examination by kidney biopsy. The total ischemic necrosis of all the elements (glomeruli, blood vessel, and tubule) of the affected area of kidney cortex is a typical histological feature of cortical necrosis.⁶ However, previous studies failed to find a correlation between kidney histopathological indices and prognosis prediction in pregnancy-associated renal cortical necrosis.¹

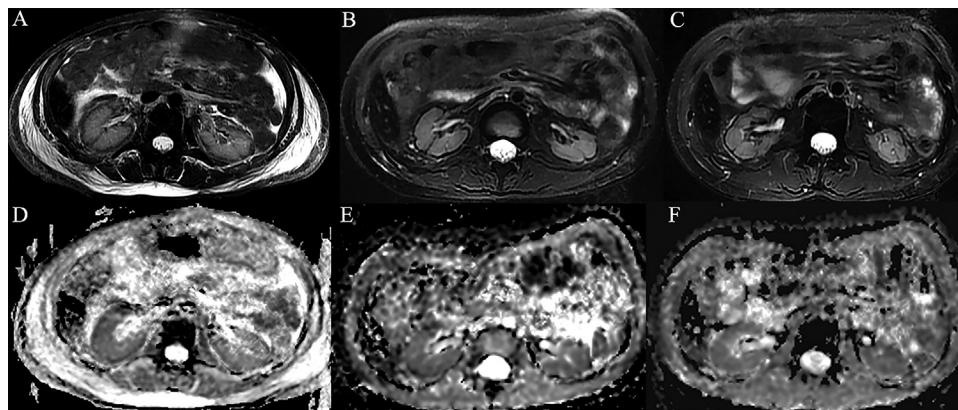


Figure 4. A 31-year-old woman, who presented with postpartum hemorrhage and acute kidney injury, was identified as atypical hemolysis uremic syndrome (aHUS). The T2-weighted image (A) obtained on the 16th day after delivery demonstrated a diffuse hypointense signal in the cortex and the column of Bertin. Serial T2-weighted images showed that the swelling cortex contour appeared to shrink 1 month (B) and 3 months (C) after the first magnetic resonance imaging (MRI) scan. The apparent diffusion coefficient (ADC) map (D) demonstrated focal hypointense signal lesions in the cortex and the column of Bertin. The corresponding serial ADC maps (E and F) disclosed that the hypointense signal in the cortex and the column of Bertin decreased gradually with the recovery of kidney function.

This probably reflects the sampling bias associated with kidney biopsy. Furthermore, invasive kidney biopsy may be contraindicated in critically ill patients, particularly those at high risk of bleeding. Jeong et al⁹ reported 8 series of MR images in 1 patient with pregnancy-associated renal cortical necrosis and 5 patients with non-pregnancy-associated renal cortical necrosis. Unfortunately, the authors did not follow-up on these patients to obtain their kidney outcomes. Francois et al⁸ reported 2 patients with cortical necrosis and suggested that MRI may be of great help for the diagnosis and follow-up of cortical necrosis, but the sample was too small. Our results showed that the imaging phenotype on T2WI might serve as a promising marker for disease severity and kidney outcome assessment. Current evidence suggests that DWI is particularly sensitive to alterations in the kidney interstitium, such as kidney fibrosis, cellular infiltration or edema, perfusion, and water handling in the tubular compartment.^{13,28-30} Cortical necrosis due to ischemia and hypoxia could result in the limited diffusion of water molecules in the cortex, and hypointense signals were observed on the ADC map. Over time, kidney cortical interstitial fibrosis developed, reflected by the negative Δ ADC value. The negative Δ ADC value, obtained by subtracting the cortical ADC from the medullary ADC value, was better correlated with kidney interstitial fibrosis than the absolute ADC in native kidney disease, transplants, and chronic kidney disease patients.^{14,31} Our study observed that the negative Δ ADC value of the KFRT subgroup was greater than that of the eGFR ≥ 60 and 15-60 mL/min/1.73 m² subgroups.

Our study had several limitations. First, the sample size of our study was small due to the rarity of pregnancy-associated renal cortical necrosis. Second, the MRI machine model and the field strength were not unified. During the 12-year study period, some MRI machines became obsolete and were replaced by new machines. In addition, the traditional DWI sequence in our study had 2 b-values of 0/50 and 800 s/mm² because of its availability, but it provided limited information (ADC only). Intravoxel incoherent motion, derived from traditional DWI, is currently recommended. Third, because of the study's retrospective nature, the timing of the MRI scan and kidney biopsy was not unified.

In conclusion, based on clinical, histological, and nonenhanced functional MRI findings of a case series of pregnancy-associated renal cortical necrosis, we found that different forms of pregnancy-associated TMA were the major causative diseases, which require the development of targeted therapies in addition to terminating the pregnancy. Nonenhanced functional MRI may provide valuable information in the diagnosis and kidney outcome assessment of cortical necrosis.

SUPPLEMENTARY MATERIAL

Supplementary File (PDF)

Figure S1: The T2-weighted images (A, C) and the apparent diffusion coefficient (ADC) maps (B, D). The cortical area was delineated

layer by layer on axial T2-weighted images (A) and summed to obtain the total cortical area. Regions of interest were placed on the cortex covering all the lesions with decreased ADC values (B).

Table S1: The Detailed MRI Scanning Sequences.

ARTICLE INFORMATION

Authors' Full Names and Academic Degrees: Rui Wang, PhD, MD, Xiang Liu, PhD, Wei Li, BM, Ying Tan, PhD, MD, Jianxing Qiu, MD, and Tao Su, MD

Authors' Affiliations: Department of Radiology, Peking University First Hospital, Beijing, China (RW, XL, WL, JQ); and Renal Division, Peking University First Hospital, Peking University Institute of Nephrology, Beijing, China (YT, TS).

Address for Correspondence: Tao Su, Renal Division, Peking University First Hospital, Peking University Institute of Nephrology, Beijing, China. Email: tao.su@bjmu.edu.cn

Authors' Contributions: Research idea and study design: RW, TS; data acquisition: RW, WL, JQ, TS, YT; data analysis/interpretation: RW, XL, JQ, TS; statistical analysis: RW, TS; supervision or mentorship: RW, TS. Each author contributed important intellectual content during manuscript drafting or revision and agrees to be personally accountable for the individual's own contributions and to ensure that questions pertaining to the accuracy or integrity of any portion of the work, even one in which the author was not directly involved, are appropriately investigated and resolved, including with documentation in the literature if appropriate.

Support: This study was funded by the National Natural Science Foundation of China (Grant Nos. 82202092), National Science and Technology Major Projects for Major New Drugs Innovation and Development (Grant 2017ZX09304028 to TS), and the Chinese Academy of Medical Sciences Innovation Fund for Medical Sciences (No. 2019-I2M-5-046). Funders supported the decision to submit for publication, but played no role in the study design, data collection, analysis, or reporting.

Financial Disclosure: The authors declare that they have no relevant financial interests.

Data Sharing: The datasets used and analyzed during this study are available from the corresponding author on reasonable request.

Peer Review: Received November 10, 2022 as a submission to the expedited consideration track with 2 external peer reviews. Direct editorial input from the Editor-in-Chief. Accepted in revised form January 20, 2023.

REFERENCES

1. Frimat M, Decambron M, Lebas C, et al. Renal cortical necrosis in postpartum hemorrhage: a case series. *Am J Kidney Dis*. 2016;68(1):50-57. doi:10.1053/j.ajkd.2015.11.022
2. Prakash J, Pant P, Singh AK, Srinivas S, Singh VP, Singh U. Renal cortical necrosis is a disappearing entity in obstetric acute kidney injury in developing countries: our three decade of experience from India. *Ren Fail*. 2015;37(7):1185-1189. doi:10.3109/0886022X.2015.1062340
3. Ramachandran R, Nayak S, Anakutti HP, et al. Postpartum renal cortical necrosis is associated with atypical hemolytic uremic syndrome in developing countries. *Kidney Int Rep*. 2019;4(3):420-424. doi:10.1016/j.ekir.2018.11.012
4. Prakash J, Vohra R, Wani IA, et al. Decreasing incidence of renal cortical necrosis in patients with acute renal failure in developing countries: a single-centre experience of 22 years from Eastern India. *Nephrol Dial Transplant*. 2007;22(4):1213-1217. doi:10.1093/ndt/gfl761

5. Beji S, Hajji M, Rais L, et al. Acute renal cortical necrosis in pregnancy: clinical course and changing prognosis. *Nephrol Ther.* 2017;13(7):550-552. doi:10.1016/j.nephro.2016.10.007
6. Bhaduarua D, Kaul A, Lal H, et al. Acute cortical necrosis in pregnancy still an important cause for end-stage renal disease in developing countries. *Saudi J Kidney Dis Transpl.* 2019;30(2):325-333. doi:10.4103/1319-2442.256839
7. Kim HJ, Cho OK. CT scan as an important diagnostic tool in the initial phase of diffuse bilateral renal cortical necrosis. *Clin Nephrol.* 1996;45(2):125-130.
8. Francois M, Tostivint I, Mercadal L, Bellin MF, Izzedine H, Deray G. MR imaging features of acute bilateral renal cortical necrosis. *Am J Kidney Dis.* 2000;35(4):745-748. doi:10.1016/s0272-6386(00)70024-2
9. Jeong JY, Kim SH, Sim JS, et al. MR findings of renal cortical necrosis. *J Comput Assist Tomogr.* 2002;26(2):232-236. doi:10.1097/00004728-200203000-00012
10. Tuttle RJ, Minielly JA. The angiographic diagnosis of acute hemorrhagic renal cortical necrosis. *Radiology.* 1978;126(3):637-638. doi:10.1148/126.3.637
11. Mamoulakis C, Tsarouhas K, Fragkiadoulaki I, et al. Contrast-induced nephropathy: basic concepts, pathophysiological implications and prevention strategies. *Pharmacol Ther.* 2017;180:99-112. doi:10.1016/j.pharmthera.2017.06.009
12. Weinreb JC, Rodby RA, Yee J, et al. Use of intravenous gadolinium-based contrast media in patients with kidney disease: consensus statements from the American College of Radiology and the National Kidney Foundation. *Kidney Med.* 2021;3(1):142-150. doi:10.1016/j.xkme.2020.10.001
13. Caroli A, Schneider M, Friedli I, et al. Diffusion-weighted magnetic resonance imaging to assess diffuse renal pathology: a systematic review and statement paper. *Nephrol Dial Transplant.* 2018;33(suppl 2):ii29-ii40. doi:10.1093/ndt/gfy163
14. Berchtold L, Crowe LA, Combescure C, et al. Diffusion-magnetic resonance imaging predicts decline of kidney function in chronic kidney disease and in patients with a kidney allograft. *Kidney Int.* 2022;101(4):804-813. doi:10.1016/j.kint.2021.12.014
15. Steiger P, Barbieri S, Kruse A, Ith M, Thoeny HC. Selection for biopsy of kidney transplant patients by diffusion-weighted MRI. *Eur Radiol.* 2017;27(10):4336-4344. doi:10.1007/s00330-017-4814-z
16. Khwaja A. KDIGO clinical practice guidelines for acute kidney injury. *Nephron Clin Pract.* 2012;120(4):c179-c184. doi:10.1159/000339789
17. Levey AS, Bosch JP, Lewis JB, Greene T, Rogers N, Roth D. A more accurate method to estimate glomerular filtration rate from serum creatinine: a new prediction equation. Modification of Diet in Renal Disease Study Group. *Ann Intern Med.* 1999;130(6):461-470. doi:10.7326/0003-4819-130-6-199903160-00002
18. Grünfeld JP, Ganeval D, Bournérias F. Acute renal failure in pregnancy. *Kidney Int.* 1980;18(2):179-191. doi:10.1038/kid.1980.127
19. Kim HJ. Bilateral renal cortical necrosis with the changes in clinical features over the past 15 years (1980-1995). *J Korean Med Sci.* 1995;10(2):132-141. doi:10.3346/jkms.1995.10.2.132
20. Brown MA, Magee LA, Kenny LC, et al. Hypertensive disorders of pregnancy: ISSHP classification, diagnosis, and management recommendations for international practice. *Hypertension.* 2018;72(1):24-43. doi:10.1161/HYPERTENSIONAHA.117.10803
21. Fakhouri F, Scully M, Provôt F, et al. Management of thrombotic microangiopathy in pregnancy and postpartum: report from an international working group. *Blood.* 2020;136(19):2103-2117. doi:10.1182/blood.2020005221
22. Prasad CB, Rathinasamy R, Kopp CR, Jain S, Jain S, Dhir V. Acute renal cortical necrosis: cortical rim sign and reverse rim sign. *Kidney Int.* 2021;100(5):1146. doi:10.1016/j.kint.2021.03.017
23. Hesp AC, Schaub JA, Prasad PV, et al. The role of renal hypoxia in the pathogenesis of diabetic kidney disease: a promising target for newer renoprotective agents including SGLT2 inhibitors? *Kidney Int.* 2020;98(3):579-589. doi:10.1016/j.kint.2020.02.041
24. Evans RG, Eppel GA, Anderson WP, Denton KM. Mechanisms underlying the differential control of blood flow in the renal medulla and cortex. *J Hypertens.* 2004;22(8):1439-1451. doi:10.1097/01.hjh.0000133744.85490.9d
25. Passmore JC, Allen RL, Hock CE, Neiberger RE. Freeze-dissection analysis of ¹³³Xe distribution to measure regional renal blood flow. *Am J Physiol.* 1983;244(5):F574-F578. doi:10.1152/ajprenal.1983.244.5.F574
26. Tuononen S, Nuutinen L, Hollmén A, Larmi TK. Renal blood flow and intrarenal oxygen tension in haemorrhagic hypotension. *Ann Chir Gynaecol Suppl.* 1977;66(5):258-261.
27. Passmore JC, Neiberger RE, Eden SW. Measurement of intrarenal anatomic distribution of krypton-85 in endotoxic shock in dogs. *Am J Physiol.* 1977;232(1):H54-H58. doi:10.1152/ajpheart.1977.232.1.H54
28. Wang W, Yu Y, Wen J, et al. Combination of functional magnetic resonance imaging and histopathologic analysis to evaluate interstitial fibrosis in kidney allografts. *Clin J Am Soc Nephrol.* 2019;14(9):1372-1380. doi:10.2215/CJN.00020119
29. Thoeny HC, De Keyzer F. Diffusion-weighted MR imaging of native and transplanted kidneys. *Radiology.* 2011;259(1):25-38. doi:10.1148/radiol.10092419
30. Berchtold L, Crowe LA, Friedli I, et al. Diffusion magnetic resonance imaging detects an increase in interstitial fibrosis earlier than the decline of renal function. *Nephrol Dial Transplant.* 2020;35(7):1274-1276. doi:10.1093/ndt/gfaa007
31. Friedli I, Crowe LA, Berchtold L, et al. New magnetic resonance imaging index for renal fibrosis assessment: a comparison between diffusion-weighted imaging and T1 mapping with histological validation. *Sci Rep.* 2016;6:30088. doi:10.1038/srep30088